COMPOSITES & POLYCON 2009
American Composites Manufacturers Association
January 15-17, 2009
Tampa, FL USA

Behavior of Full-Scale Concrete Columns Internally Reinforced with Glass FRP Bars under Pure Axial Load

by

Antonio De Luca
Fabio Matta
Antonio Nanni
Department of Civil, Architectural and Environmental Engineering, University of Miami

Abstract

Glass fiber reinforced polymer (GFRP) bars are a viable option as reinforcement in concrete, particularly when corrosion resistance or electromagnetic transparency are sought. However, the behavior of GFRP bars in compression members is a relevant issue that still needs to be addressed. This paper presents a pilot research that includes experimental testing of full-scale square GFRP and steel reinforced concrete (RC) columns under pure axial load. The objectives were to demonstrate whether the compressive behavior of GFRP bars impacts the column response, and to understand whether the contribution of GFRP ties to column confinement enables to prevent instability of the longitudinal bars. Five specimens were tested: one was a benchmark steel RC column, the others were GFRP RC columns. The GFRP RC specimens were subdivided into two sets of two, each set identical to the other, but using bars from two different manufacturers. The steel RC specimen was constructed using the ACI 318-05 code-mandated minimum amount of longitudinal reinforcement, and minimum tie area at maximum spacing. Each set of GFRP RC specimens had the same amount of longitudinal reinforcement as the steel RC benchmark, and two different spacings of transverse reinforcement.

All the GFRP RC specimens provided similar strength to that of the steel RC specimen. The failure mode was strongly influenced by the spacing of the GFRP ties. The outcomes of this research are a much needed contribution to the development of rational design criteria for longitudinal and transverse GFRP reinforcement.

Background

The corrosion resistance, high strength and light weight of glass fiber reinforced polymer (GFRP) bars, together with their transparency to electrical and magnetic fields, ease of manufacturing, and ease of installation, have made them a competitive option as reinforcement in concrete. The use of GFRP reinforcement is particularly attractive for structures that operate in aggressive environments, such as in coastal regions, or for buildings supporting magnetic resonance imaging (MRI) units or other equipment sensitive to electromagnetic fields. However, the behavior of GFRP bars as longitudinal reinforcement in reinforced concrete (RC) compression members is still a relevant issue that needs to be addressed.

The compressive strength of GFRP bars was found to be 55% lower than the tensile strength by Mallick (1988) and Wu (1990). Different modes of failure (transverse tensile failure, fiber microcracking or shear failure) may characterize the response of the fiber reinforced polymer (FRP) bars in compression, depending on the type of fibers, the fiber-volume fraction, and the type of resin. According to Mallick (1988) and Eshani (1993), the compressive modulus of elasticity of GFRP rebars is approximately 80% of the tensile modulus.

To date, very few studies have been conducted that included laboratory experiments on small-scale concrete columns reinforced with FRP bars. In particular, Alsayed et al. (1999) investigated the effect of replacing longitudinal and lateral steel reinforcing bars by an equal amount of GFRP bars. Based on the results of tests performed on small-scale columns under concentric loads, it was reported that replacing longitudinal steel reinforcing bars with GFRP bars reduced the axial capacity of the columns by on average 13%. It was observed that, irrespective of the type of longitudinal bars, replacing steel ties with GFRP ties reduced the axial capacity of the column by about 10%. Moreover, replacing steel ties with GFRP ties had no influence on the load-deflection response of the columns up to approximately 80% of the ultimate capacity. Almusallam et al. (1997) studied the effect of different ratios of compression reinforcement on the behavior of concrete beams reinforced with GFRP bars and indicated that the GFRP compression reinforcement has insignificant influence on the behavior of all tested beams.

Significance

Except for the Japan Society of Civil Engineers (Sonobe et al. 1997b) that has established a design procedure specifically for the use of FRP reinforcement in RC columns, current guidelines and codes of practice such as in the United States (ACI 440 2006), in Canada

(CSA 2002) and in Italy (CNR 2006), do not recommend the use of FRP bars as reinforcement in compression.

Full-scale experiments are very critical to validate the technology, and to understand the mechanics to underpin rational design methodologies.

Objectives

The scope of the research reported herein was to validate the use of GFRP bars as internal reinforcement for RC columns subjected to concentric compressive loads. In particular, this study aims at: investigating the impact of the compressive behavior of longitudinal GFRP bars on the column performance; understanding the contribution of GFRP ties to confinement and to prevent instability of the longitudinal GFRP reinforcement; and assessing the independence of the column performance from the specific GFRP bars used.

Based on this research, new evidence and modified language may be proposed to improve design criteria for compression members in terms of definition of longitudinal and transverse reinforcement.

Experimental Program

The research program included laboratory testing of full-scale GFRP and steel RC columns under pure axial load. The study was undertaken using 10.0 ft (3.0 m) long specimens of square cross-section with a 2.0 ft (0.6 m) side. The test matrix is shown in Table 1. Two different GFRP bar types were used and are herein denoted as Bar A (Figure 1) and Bar B (Figure 2). Both bar types have the same nominal cross-section and different surface preparation: deformed shape using helicoidal wraps for Bar A, and sand coating for Bar B.

Five specimens were tested: a steel RC column used as benchmark, and four GFRP RC columns. The GFRP RC columns were subdivided into two sets of two, each set identical to the other, but using Bar A and Bar B, respectively. The purpose of the duplication is to show that different GFRP bar qualities have similar response. The RC column using steel bars was designed and constructed using the minimum amount of longitudinal reinforcement and the minimum tie cross-sectional area at maximum spacing as mandated by ACI 318-05 (ACI 2005) in Section 10.9.1 and Section 7.10.5.2, respectively. In particular, the total area of longitudinal bars was taken as 1.0% of the gross section area, A_g, and eight No. 8 (25.4 mm diameter) bars were chosen; No. 4 (12.7 mm diameter) ties were used at a spacing of 16 in (406 mm) on center. For each set of two GFRP RC columns, bar size and total area of longitudinal reinforcement was adopted as for the steel case. For the GFRP ties, the same bar size was used, but the spacing was reduced to 12 in (305 mm) and 3 in (76 mm) when compared to the steel case. The 12-inch (305-mm) spacing has been defined to prevent longitudinal bars buckling, while the 3-inch (76-mm) spacing has been chosen as the minimum practical spacing for GFRP ties.

Specimen Construction

Figure 3 through Figure 5 show the reinforcement layout of the column specimens. The cross-section layout is identical for all the specimens. No. 4 (12.7 mm diameter) cross-ties were used in order to provide additional lateral support to the longitudinal bars. Plastic zip ties were used to hold together the GFRP bars. GFRP ties were made assembling together two C-shaped No. 4 bars overlapping the two braces of the C-shape. The two-piece-assembled GFRP ties were staggered along the column cage in order to avoid having the overlapped braces on the same side for two consecutive tie layers. No. 4 (12.7 mm diameter) 2-inch (50.8-mm) spaced steel ties were used at the two ends of the specimens to preclude any premature failure because of the concentration of stresses due to the application of the load. During the assembling of the reinforcement (steel and GFRP) cages strain gages were installed on selected longitudinal bars and ties. Wood formworks were used to cast the specimens. Concrete was poured while the formwork was laying horizontally on the ground. Before pouring concrete, two hooked-shaped pick-up points were embedded in the cages.

Materials

A nominal 5,000-psi concrete mix design was used with a water-cement ratio equal to 0.53 and unit weight of 140.8 lb/ft^3 (22.1 kN/m^3). Column specimens were cast one at the time using different concrete batches. The concrete strength for each batch was based on six 6-inch by 12-inch (152-mm by 304-mm) cylinder samples. Table 2 shows the average and the standard deviation of the compressive strength per each specimen. ASTM Grade 60 steel was used. The steel was characterized by minimum yield strength of 60 ksi (414 MPa) and modulus of elasticity of 29 msi (200 GPa). Properties of the GFRP bars were provided by the manufacturers as shown in Table 3.

Test Setup and Test Procedure

The tests were conducted using a 5 Million Pound (22,250 kilo Newton) Universal Testing Machine (Figure 6) at the Fritz Engineering Laboratories at Lehigh University (Bethlehem, PA). When ready to be tested, the column specimen was raised in vertical position with the use of a crane and wheeled to the machine on a pallet jack. Once placed in the machine, the specimen was hanged to the head of the machine (Figure 7). Special care was taken that the column specimen was directly at the center of the machine and that was plumb (Figure 8). To assure uniformity and concentricity of the applied

load, bottom and top surfaces of the column specimens were hydro-stoned. While the specimen was held in the proper position in the center of the machine, a thin layer of hydro-stone paste was spread upon the bearing plate placed on the base of the machine and below the specimen (Figure 9). Afterward, the specimen was lowered and placed on the hydro-stone layer. The hydro-stone paste was then spread also on the top surface of the specimen. The head of the machine was run down and a compressive load of about 10 kips (44.5 kN) was applied to allow the hydro-stone to set (Figure 10).

Once the specimen was installed in the machine and the specimen surfaces were hydro-stoned, the external sensors (strain gages and LVDTs) were installed and connected to the data logger and balanced (Figure 11). Two different types of strain gages were used: 0.197 in (5 mm) strain gages were installed onto the internal reinforcement; and 1.969 in (50 mm) strain gages were used for the concrete. A total of eight LVDTs were used: four were installed to measure vertical displacements and four to measure transverse deformations.

The load was applied concentrically under a displacement control rate of 0.02 in/min (0.5 mm/min). The loading was conducted in five or six cycles in increments of 500 kips (2,225 kN). Upon reaching 75% of the expected maximum capacity, the displacement control rate was reduced to 0.012 in/min (0.3 mm/min) in order to obtain a detailed record of the post-peak response of the specimen. Each test lasted about 5 hours.

Test Results

The behavior of all column specimens up to failure was very similar. The failure mechanism was usually initiated by vertical cracks followed, first, by lateral deflection of the vertical bars resulting in splitting of the concrete cover and, finally, by crushing of the concrete core and buckling of the vertical reinforcing bars.

For all the specimens, when the maximum load was reached, the averaged stress (defined as the ratio between the maximum load applied and the gross sectional area) reached about the 90% of the average concrete strength.

In particular, for the control specimen and for the large spaced ones (S-16, A-12 and B-12), with the lowering of the head of the machine after the maximum load had been reached, the concrete broke out accompanied by buckling of the vertical bars. The failure was sudden and, in the case of specimen A-12 and B-12, an explosive noise accompanied the crushing.

In the case of the small spaced specimens (A-3 and B-3), after attaining the peak load, the lowering of the head of the machine produced large vertical deformation without crushing the concrete core because of the confinement action offered by the small tie spacing.

Test results are summarized in Table 4. The average peak stress is evaluated as the peak load divided by the gross sectional area of the specimen. The ratio between the average peak stress and the cylinder average strength is also reported. Figure 12 compares the behavior of all the specimens in terms of normalized stress and average axial shortening. Figure 13 and Figure 14 compare the control specimen with Bar A and Bar B 3-in (76-mm) tie spacing specimens and with Bar A and Bar B 12-inch (305-mm) tie spacing, respectively. Figure 15 through Figure 18 show some details of specimen failures.

Conclusions

Specimens internally reinforced with GFRP bars behaved very similar to the conventional steel reinforced one. The normalized strength (maximum load normalized with respect to the cylinder strength multiplied by the gross sectional area of concrete cross-section) reached about the same level for all specimens. 12-inch (305-mm) tie spacing GFRP specimens failed in more brittle mode (no premonition at all). On the other side, 3-inch (76-mm) tie spacing GFRP specimens experienced a ductile failure. The quality of the bars did not affect performance.

Based on the test results presented, it can be concluded that use of FRP as compression reinforcement is not detrimental for column performance and may be allowed when design is for only vertical loads even though the FRP contribution to compressive strength should be neglected in the computation of the ultimate axial load capacity. The tie spacing plays a relevant role in terms of ductility: a brittle failure can and should be prevented by using a small spacing of the ties. Research is undertaking to develop a design criterion to minimize the brittle failure.

Acknowledgments

The authors gratefully acknowledge the support of the NSF Industry/University Cooperative Research Center for "Repair of Buildings and Bridges with Composites" (RB^2C) at the University of Miami, and of the RB^2C industry members Hughes Brothers, Inc., and Pultrall, Inc. Special thanks are extended to the Fritz Engineering Laboratory at Lehigh University, and in particular to Mr. Frank Stokes and Mr. Gene Matlock, for the assistance in planning and conducting the tests.

Authors:

Antonio De Luca is a Graduate Research Assistant at the Department of Civil, Architectural, and Environmental Engineering at the University of Miami. His research focuses on the use of advanced composite material systems as internal and external reinforcement in concrete columns. E-mail: adeluca@umiami.edu.

Fabio Matta is a Research Assistant Professor at the Department of Civil, Architectural, and Environmental Engineering at the University of Miami. His research interests include the use of advanced materials for the internal and external reinforcement of concrete.

Antonio Nanni is the Lester and Gwen Fisher Endowed Scholar, Professor and Chair at the Department of Civil, Architectural, and Environmental Engineering at the University of Miami. His research interests include the evaluation, repair and rehabilitation of concrete structures.

References

ACI Committee 318, 2005, "Building Code Requirements for Structural Concrete (ACI 318-05) and Commentary (318R-05)," American Concrete Institute, Farmington Hills, MI, 430 pp.

ACI Committee 440, 2006, "Guide for the Design and Construction of Structural Concrete Reinforced with FRP Bars (ACI 440.4R-06)," American Concrete Institute, Farmington Hills, MI, 44 pp.

Almusallam, T. H.; Al-Salloum, Y.; Alsayed, S.; and Amjad, M., 1997, "Behavior of Concrete Beams Doubly Reinforced by FRP Bars," *Proceedings of the Third International Symposium on Non-Metallic (FRP) Reinforcement for Concrete Structures (FRPRCS-3)*, Japan Concrete Institute, Tokyo, Japan, V. 2, pp. 471-478.

Alsayed, S. H.; Al-Salloum, Y. A.; Almusallam, T. H.; and Amjad, M. A, 1999, "Concrete Columns Reinforced by GFRP Rods," *Fourth International Symposium on Fiber-Reinforced Polymer Reinforcement for Reinforced Concrete Structures* , SP-188, C. W. Dolan, S. H. Rizkalla, and A. Nanni, eds., American Concrete Institute, Farmington Hills, Mich., pp. 103-112.

CAN/CSA-S6-02, 2002, "Design and Construction of Building Components with Fibre-Reinforced Polymers," CAN/CSA S806-02, Canadian Standards Association, Rexdale, Ontario, Canada, 177 pp.

CNR Advisory Committee on Technical Recommendations for Construction, 2006, "Guide for the Design and Construction of Concrete Structures with Fiber-Reinforced Polymer Bars," CNR-DT 203/2006, National Research Council, Rome, Italy, 39 pp.

Ehsani, M. R., 1993, "Glass-Fiber Reinforcing Bars," *Alternative Materials for the Reinforcement and Prestressing of Concrete*, J. L. Clarke, Blackie Academic & Professional, London, pp. 35-54.

Mallick, P. K., 1988, *Fiber Reinforced Composites, Materials, Manufacturing, and Design*, Marcell Dekker, Inc., New York, 469 pp.

Sonobe, Y.; Fukuyama, H.; Okamoto, T.; Kani, N.; Kimura, K.; Kobatashi, K.; Masuda, Y.; Matsuzaki, Y.; Mochizuki, S.; Nagasaka, T.; Shimizu, A.; Tanano, H.; Tanigaki, M.; and Teshigawara, M., 1997b, "Design Guidelines of FRP Reinforced Concrete Building Structures," *ASCE Journal of Composites for Construction,* V. 1, No. 3, pp. 90-115.

Wu, W. P., 1990, "Thermomechanical Properties of Fiber Reinforced Plastic (FRP) Bars," PhD dissertation, West Virginia University, Morgantown, W.Va., 292 pp.

Figures

Figure 1 – Detail of Bar A type

Figure 2 – Detail of Bar B type

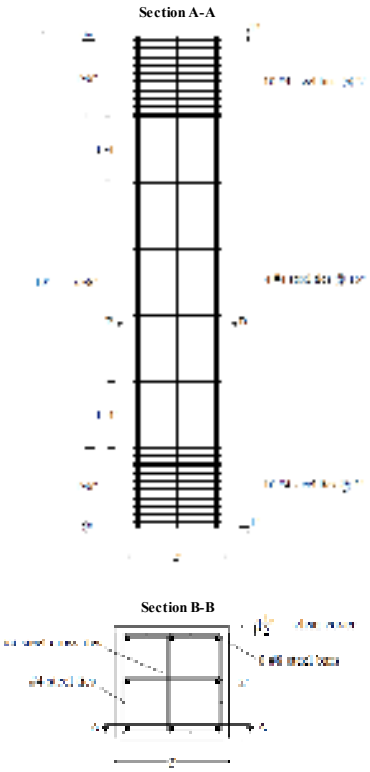

Figure 3 – Steel RC column specimen schematic

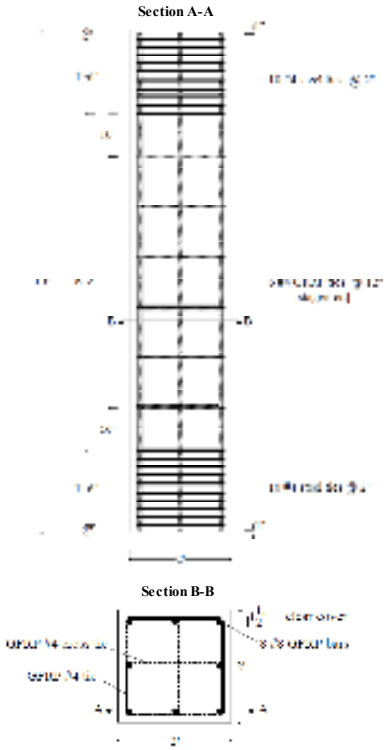

Figure 5 – GFRP RC column specimen schematic: large spacing

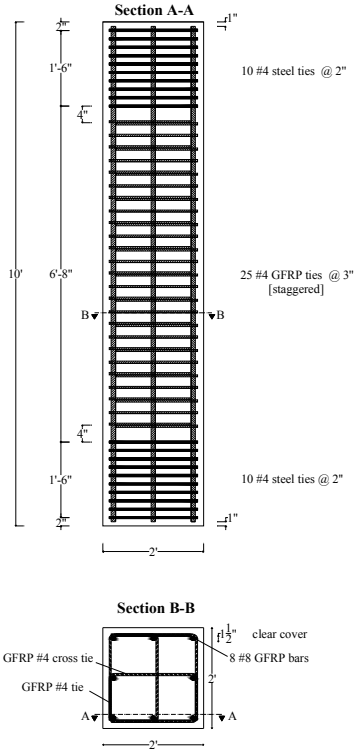

Figure 4 – GFRP RC column specimen schematic: small spacing

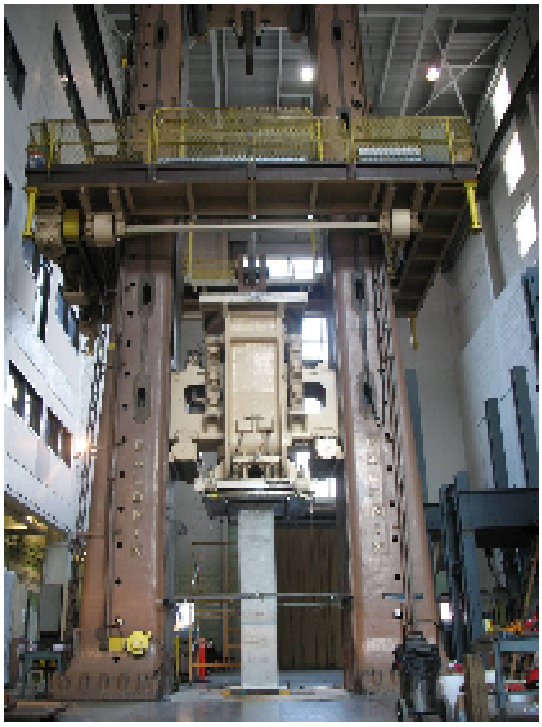

Figure 6 – Test setup

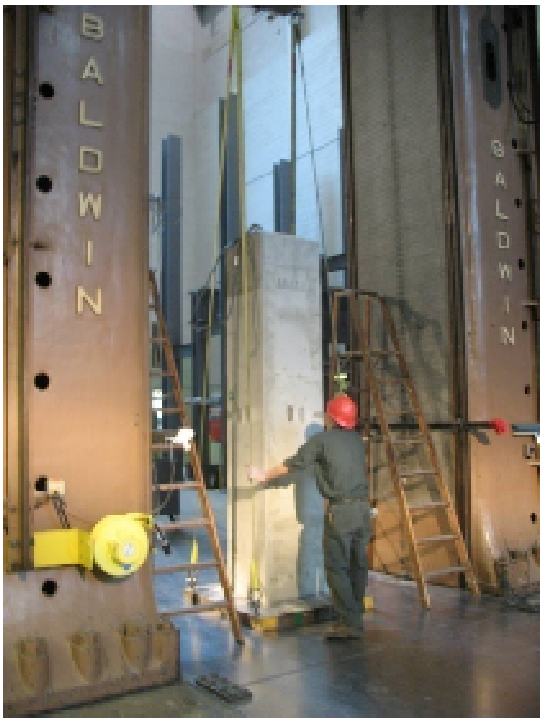

Figure 7 – Column specimen centered in the machine

Figure 8 – Column specimen centered and plumbed

Figure 9 – Hydro-stoning of the bottom surface

Figure 10 – Hydro-stoning of the top surface

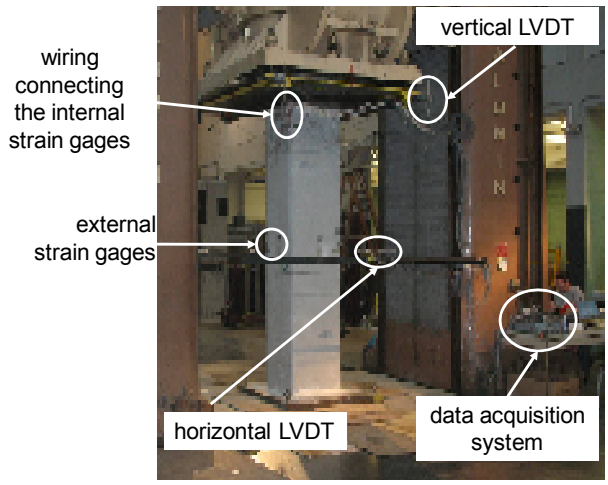

Figure 11 – Instrumentation

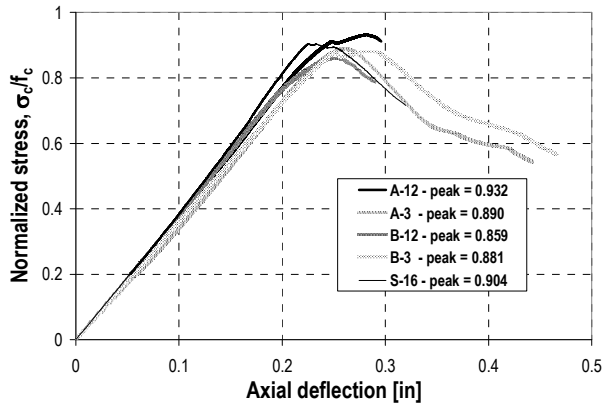

Figure 12 – Comparison: Bar A and Bar B 3-inch and 12-inch tie spacing specimens with Benchmark

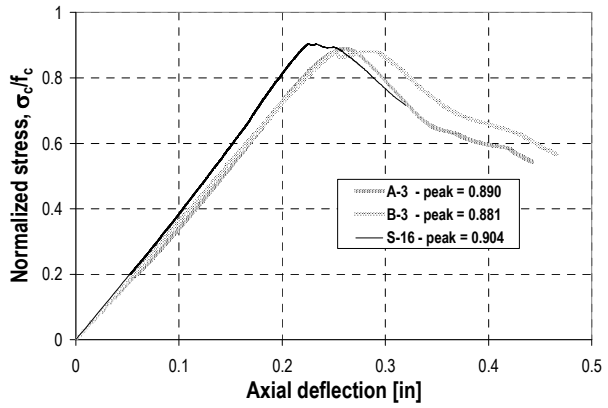

Figure 13 – Comparison: Bar A and Bar B 3-inch tie spacing specimen with Benchmark

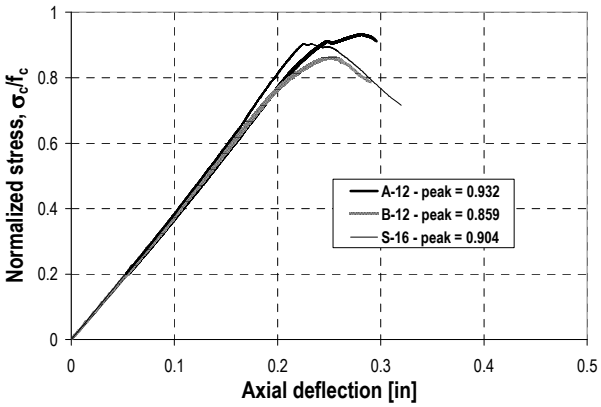

Figure 14 – Comparison: Bar A and Bar B 12-inch tie spacing specimen with Benchmark

Figure 15 – Bar A 3-inche tie spacing: failure detail

Figure 16– Bar B 3-inche tie spacing: failure detail

Figure 17 – Bar A 12-inch tie spacing: failure detail

Figure 18 – Bar B 12-inch tie spacing: failure detail

Tables:

Table 1 – Test Matrix

Square column 24x24 in [610x610 mm]		Specimen code	Longitudinal reinforcement	Transverse reinforcement
Steel RC column benchmark with 16-inch (406-mm) tie spacing		S-16	8 #8 bars	#4 ties @ 16'' (@ 406 mm)
Bar A column with 12-inch (305-mm) tie spacing	same volume of longitudinal reinforcement as for steel [ρ_{min} = 1%]	A-12	8 #8 bars	#4 ties @ 12'' (@ 305 mm)
Bar B column with 12-inch (305-mm) tie spacing		B-12	8 #8 bars	#4 ties @ 12'' (@ 305 mm)
Bar A column with 3-inch (76-mm) tie spacing		A-3	8 #8 bars	#4 ties @ 3'' (@ 76 mm)
Bar B column with 3-inch (76-mm) tie spacing		B-3	8 #8 bars	#4 ties @ 3'' (@ 76 mm)

Table 2 – Concrete strength (from concrete cylinders)

Specimen code	Average compressive strength, f_c (psi) [MPa]	Standard deviation (psi) [MPa]
S-16	5,413 (37.32)	352 (2.43)
A-12	6,340 (47.31)	307 (2.12)
B-12	5,885 (40.58)	345 (2.38)
A-3	5,236 (36.10)	204 (1.41)
B-3	4,763 (32.84)	295 (2.03)

Table 3 – GFRP longitudinal bar properties provided by the manufacturer (from testing of the bar lots)

	Bar type	
Parameter	**Type A**	**Type B**
Bar size – Area (in^2) [mm^2]	#8 – 0.503 (324)	#8 – 0.503 (324)
Ultimate strain (%)	1.38	1.60
Modulus of elasticity (psi) [GPa]	6,405,294 (44.16)	6,440,000 (44.40)
Tensile strength (psi) [MPa]	88,179 (608)	103,300 (712)

Table 4 – Test results

Specimen	Cylinder average strength, f_c (psi) [MPa]	Peak load, P_u (kips) [kN]	Average peak stress, σ_c (psi) [MPa]	$(\sigma_c/f_c)_{peak}$
S-16	5,413 (37.32)	2,818 (12,500)	4,892 (33.73)	90 %
A-12	6,340 (47.31)	3,415 (15,190)	5,929 (40.88)	93 %
B-12	5,885 (40.58)	2,911 (12,950)	5,054 (34.85)	86 %
A-3	5,236 (36.10)	2,681 (11,930)	4,654 (32.09)	89 %
B-3	4,763 (32.84)	2,417 (10,750)	4,196 (28.93)	88 %